JOURNAL OF THERMOPHYSICS AND HEAT TRANSFER
Vol. 9, No. 2, April–June 1995

Non-Kirchhoff Surface Using Media with Direc onally Varying Absorption Efficiency

Peter D. Jones* and Daniel W. Mackowski*
Auburn University, Auburn, Alabama 36849

A unique radiation trapping surface is proposed in which the effective monochromatic absorptivity-to-emissivity ratio is much greater than one (a non-Kirchhoff surface). The surface is comprised of a plane-parallel layer of a disperse suspension of compound particles. Each particle has a small absorber sphere embedded eccentricly in a larger lens sphere, resulting in an absorption coefficient for the medium that is highly dependent on direction. In combination with an opaque, specularly reflecting boundary opposite the incident flux side of the medium, such a device acts as a planar radiation trap. Computational results show that an effective monochromatic absorptivity-to-emissivity ratio of up to 70 can be achieved, along with a through-flux that is superior to that of an opaque surface that obeys Kirchhoff's law. The effects of optical thickness, incidence angle, particle orientation error, and suspending substrate conductivity are investigated.

Nomenclature

d_p = compound particle diameter, m
I = radiative intensity, W/m²sr
I_b = blackbody intensity, W/m²sr, $\sigma_b T^4/\pi$
I^* = dimensionless intensity, $I/(\sigma_b T_0^4/\pi)$
J = spatial mesh size
j = spatial discretization index
k = medium effective thermal conductivity, W/mK
M = directional polar mesh size, twice quadrature order
m = directional polar discretization index
N = directional azimuthal mesh size
N_p = compound particle number density, m^{-3}
N_s = Stark number or conduction-to-radiation ratio, $k\beta/4\sigma_b T_0^3$
n = directional azimuthal discretization index
Q_a = compound particle absorption efficiency, directionally dependent
Q_e = compound particle extinction efficiency, $Q_a + Q_s$, constant
Q_s = compound particle scattering efficiency, directionally dependent
q = net total heat flux, W/m²
q_0 = incident collimated radiative flux, W/m²
r = spatial location vector, m
s = interparticle spacing, m
$\hat{s}$ = directional unit vector
$\hat{s}'$ = compliment to directional unit vector
T = temperature, K
T_w = temperature at the collecting surface, K
T^* = temperature linearization point, K
T_0 = reference temperature, K, $(q_0/\sigma_b)^{1/4}$
w_m = directional polar quadrature integration weight
w_n = directional azimuthal quadrature integration weight
y = spatial coordinate, m
y_{max} = layer thickness, m
α = effective absorptivity
β = extinction coefficient, m^{-1}, $Q_e \pi d_p^2 N_p/4$
Γ = dimensionless temperature, T/T_0
Γ_w = dimensionless temperature at the collecting surface
γ = absorber sphere diameter to lens sphere diameter ratio
ε = effective emissivity
ζ = dimensionless heat flux, q/q_0
ζ_w = dimensionless heat flux at the collecting surface
Θ = scattering angle
θ = directional polar angle
θ_c = incidence angle
κ = absorption coefficient, m^{-1}, $Q_a \pi d_p^2 N_p/4$
λ = wavelength, m
ρ^s = collecting surface sp ar reflectivity
σ_b = Stefan-Boltzmann c nt, 5.67×10^{-8} W/m²
σ_s = scattering coefficie $^{-1}$, $Q_s \pi d_p^2 N_p/4$
τ = optical spatial coo βy
τ_0 = optical thickness,
Φ = scattering phase fu
Ω = solid angle, sr

Received June 15, 1994; revision received Sept. 9, 1994; accepted for publication Sept. 12, 1994. Copyright © 1994 by the American Institute of Aeronautics and Astronautics, Inc. All rights reserved.

*Assistant Professor, Mechanical Engineering Department. Member AIAA.

Int on

MACKOWSKI and J troduced a unique, hypothetical compound p in which a small sphere of radiatively absorbing materi bedded eccentrically within a larger sphere of refracti lens material. Solution of Maxwell's wave equations is compound particle yield the prediction of highly dir l absorption and scattering efficiencies (e.g., Fig. 1). T npound particles are highly absorbing of radiative inten om a narrow band of directions, and essentially nonab ng from all other directions. In order to examine the po al application of these compound particles, a configurat is proposed in this article in which a disperse assembly of c mpound particles is suspended in a conducting, radiatively nonparticipating substrate to form a particulate medium. If the particles can be organized to all have the same orientation (i.e., the eccentrically located absorber sphere is similarly oriented in each compound particle of the particulate medium, as in Fig. 2), then this medium will also have directionally-dependent absorption and scattering characteristics. Analysis of this medium requires a specialized form of the radiative transfer equation (RTE), and a solution methodology that may be applied to media with directionally varying absorption and scattering coefficients. These techniques are applied to analyze the thermal behavior of a slab of this substrate/compound particle medium in operation as a radiation trapping surface.

The goal of this article is to determine if there is sufficient potential benefit from the use of compound particles in this medium to warrant compound particle optimization studies and investigation of techniques for actually fabricating the

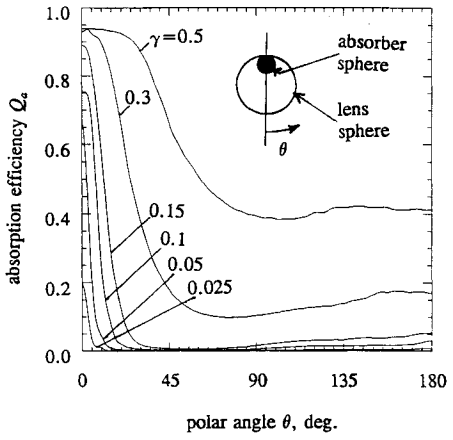

Fig. 1 Absorption efficiency as function of incidence angle; after Mackowski and Jones.[1]

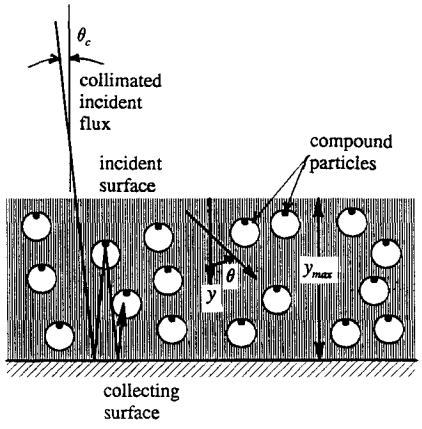

Fig. 2 General features of plane parallel substrate/disperse compound particle radiation trap.

compound particles. While no specific materials or manufacturing techniques for the compound particles are advanced in this article, it may be that differences in physical and electrical properties between the lens sphere and the eccentrically embedded absorber sphere will lead to development of a manufacturing strategy providing uniform orientation of the compound particles to within a Gaussian error.

An idealized radiation trap employing a finite thickness collecting surface comprised of a substrate/compound particle medium is shown in Fig. 2. The medium is comprised of a substrate of radiatively nonparticipating material in which compound particles have been embedded so that their absorbing side faces a collecting surface. The collecting surface is an opaque specular reflector. Some portion of the incident solar intensity will transmit through the substrate/particle medium, reflect on the collecting surface, and become reincident on the medium from the opposite direction. Absorption is high from this direction, and the original incident intensity has a tendency to become trapped between the higher absorption/emission side of the particles and the reflecting collecting surface. A high temperature in the medium results from this trapping effect. Heat may be drawn from this high-temperature reservoir by conduction across the collecting surface, and carried away by any convenient heat exchange mechanism on the opposite side of the collecting surface.

The device thus configured acts as a surface of high effective absorptivity and low effective emissivity (a non-Kirchhoff surface), in that at equilibrium the device attains a higher temperature than would be attained by a surface with an absorptivity-to-emissivity ratio of unity. Absorptivity exceeds emissivity in this device without regard to wavelength, whereas conventional planar solar absorption surfaces achieve high total absorptivity and low total emissivity by matching the spectral variations in surface emissivity so that its value is high in the incidence wavelengths and low in the collecting surface temperature blackbody emission wavelengths. Therefore, the device presently considered acts as a unique spectrally non-Kirchhoff surface, in that Kirchhoff's law does not apply on even a spectral basis, and achieves an effective absorptivity to emissivity ratio greater than unity without regard to the spectral distributions of incident and emitted power. It must be noted that the present work deals only with an augmented one-dimensional surface (i.e., extending uniformly to infinity in dimensions other than thickness), which may trap, or fail to emit, intensity much more effectively than any surface on which Kirchhoff's law is obeyed. The compound particle medium is not considered to be a complete absorption system, but rather an enhanced surface that may be a component of such a system.

Quantifying the performance of the proposed substrate/compound particle medium device depends upon solution of the RTE with directionally varying absorption and scattering coefficients. Directional variation of scattering and absorption coefficients is almost never considered in radiation heat transfer studies, although such effects may have an important impact on heat transfer in fixed solid matrices, such as foam ceramics.[2] Two problems in which directionally varying absorption and scattering coefficients have been considered are 1) heat transfer through fibrous matrices and 2) sunlight transmission through leaf canopies. In the fibrous matrix problem, directionally varying scattering arises from the varying tilt with which a ray of intensity meets a cylindrical fiber surface. Lee[3-5] has considered the combined effect of scattering coefficient and scattering phase function to determine the total scattered intensity distribution for regularly and randomly oriented arrays of cylindrical fibers. Chern et al.[6] have considered these effects as part of an overall heat transfer model for fabrication of tape-wound composite shells. The appearance of directionally-dependent scattering in the leaf canopy problem is due to the difference in radiative surface properties between the front and back of typical leaves, and the orientational distribution of leaves in the canopy. Both Marshak[7] and Shultis and Myneni[8] have modeled this problem as a cold medium, combining the scattering coefficient and scattering phase function, and obtaining solutions by both functional approximation of the scattering combination and the discrete ordinates method. Further detail is given in Ref. 9. In the following analysis, the RTE and energy equations are developed for a plane parallel slab of substrate/compound particle medium with an incident flux inclined from the normal. This model is solved using the discrete ordinates method and a finite volume central difference approach to examine the performance of the medium under different boundary conditions and parameter variations.

Analysis

A section of slab of conducting, radiatively nonparticipating material, in which a monodisperse array of compound particles is suspended, is shown in Fig. 2. The incident surface is transparent (or open), and thus, incident (solar) intensity impinges directly into the medium. The environment on the incident side is taken to be a cold vacuum (space) in order to avoid consideration of environmental conditions on the performance of the substrate/compound particle medium. The opposite side of the medium is bounded by an opaque surface, taken to be specularly reflecting and diffusely emitting. A representative radiation path is shown to suggest the intensity trapping effect. The incident ray transmits through the medium (subject to extinction), and then engages in a sequence of reflections from the collecting surface, absorption by particles, emission by particles, reflection from the surface, etc.

Heat transfer in this medium is analyzed by numerical solution of the energy equation and RTE, subject to the following assumptions:

1) The incident radiation is collimated at an angle θ_c to the surface.

2) The far-field environment on the incident side of the medium is a cold vacuum. The far field on the collecting surface side of the medium is perfectly opaque, and either a fixed temperature or a fixed heat flux boundary condition may be applied at the collecting surface.

3) All intensities and radiative properties are spectrally averaged (gray). This assumption is taken primarily to separate the effects of directional absorption and scattering from those of the spectral properties of specific materials. In reality, the absorption and scattering coefficients and the scattering phase function are related to the particle size parameter $\pi d_p/\lambda$ and the spectral indices of refraction of the various materials. As long as the size parameter is large, i.e., 30 or more, there is little variation in directional distribution of absorption coefficient with increasing size parameter.[1] This limit corresponds to smaller particles ($d_p >$ 100 μm) than probably can be manufactured, and so dependence on size parameter is neglected. Indices of refraction are also wavelength-dependent for real materials, although here only hypothetical materials with constant indices of refraction are considered in order to yield general, order of magnitude results that are not specific to species or temperature range.

4) The substrate is conductive and transparent with an index of refraction of unity. Conduction may be summarized by Fourier's law and a suitable thermal conductivity for this disperse two-phase medium.

5) The particles scatter independently. For the large-size parameters considered here, Drolen and Tien (as reported by Modest[10]) conclude that dependent scattering effects are not significant until the particle number density increases nearly to the point of a packed bed. Mackowski and Jones[1] find that there is little difference between the scattering phase function calculated (using Lorenz/Mie theory) for the lens sphere alone, and for the lens sphere with an embedded absorber sphere. It is found in the following analysis that the results have very little sensitivity to the form of the scattering phase function. Therefore, the scattering phase function is represented as that of a single lens sphere alone.

6) The collecting surface is opaque, specularly reflecting, and diffusely emitting.

The RTE is derived by considering the change $\mathrm{d}I$ of an intensity I as it travels a distance $\mathrm{d}s$ in a direction $\hat{s}$. This change is made up of absorption from the direction $\hat{s}$, $(\mathrm{d}I)_{\mathrm{abs}} = -\kappa(\hat{s}')I(\boldsymbol{r}, \hat{s})$, scattering out of the direction $\hat{s}$, $(\mathrm{d}I)_{\mathrm{scat,out}} = -\sigma_s(\hat{s}')I(\boldsymbol{r}, \hat{s})$, emission into the direction $\hat{s}$, $(\mathrm{d}I)_{\mathrm{em}} = \kappa(\hat{s})I_b(\boldsymbol{r})$, and scattering into the direction $\hat{s}$

$$(\mathrm{d}I)_{\mathrm{scat,in}} = \frac{1}{4\pi}\int_{4\pi} \sigma_s(\hat{s}_i')I(\boldsymbol{r}, \hat{s}_i)\Phi(\hat{s}_i, \hat{s})\,\mathrm{d}\Omega_i \tag{1}$$

where $\sigma_s(\hat{s}_i')$ represents the portion of the intensity in direction $\hat{s}_i$ that is scattered, and $\Phi(\hat{s}_i, \hat{s})$ represents the portion of this scatter that is directed along $\hat{s}$. Note the use of the complimentary direction $\hat{s}'$. Figure 1 defines the absorption efficiency in its emissive sense. It is assumed that Kirchhoff's law holds on the compound particle on a directional basis, with the absorption coefficient from a particular point source equaling the emission coefficient towards that point source. Therefore, e.g., the particle shown in Fig. 1 would have high emission in the $\theta = 0$ direction, and would highly absorb intensity coming from the $\theta = 180$-deg direction.

Following the technique of Kim and Lee[11] in expressing collimated incident flux effects (as demonstrated by Modest[10]), the fully directionally-dependent form of the RTE may then be written

$$\begin{aligned}\hat{s}\cdot\nabla I(\boldsymbol{r}, \hat{s}) + [\kappa(\hat{s}') + \sigma_s(\hat{s}')]I(\boldsymbol{r}, \hat{s}) &= \kappa(\hat{s})I_b(\boldsymbol{r}) \\ &+ \frac{1}{4\pi}\int_{4\pi} \sigma_s(\hat{s}_i')I(\boldsymbol{r}, \hat{s}_i)\Phi(\hat{s}_i, \hat{s})\,\mathrm{d}\Omega_i \\ &+ \frac{\sigma_s(\hat{s}_c')}{4\pi} q_0 e^{-\tau/\mu_c}\,\Phi(\hat{s}_c, \hat{s}) \\ &+ \rho^s \frac{\sigma_s(\hat{s}_r')}{4\pi} q_0 e^{-(2\tau_0-\tau)/\mu_c}\,\Phi(\hat{s}_r, \hat{s})\end{aligned} \tag{2}$$

where $\hat{s}_c$ is the direction of the incident flux, $\hat{s}_r$ is the specularly reflected direction from the collecting surface, and I is taken to be the diffuse (as opposed to collimated) contribution to total intensity. Rewriting for a plane parallel medium, and making use of Mackowski and Jones[1] finding that the overall extinction efficiency for the compound particles is constant with direction, results in

$$\begin{aligned}\cos\theta\frac{\partial I(y, \theta, \psi)}{\partial y} + \beta I(y, \theta, \psi) &= \kappa(\theta)I_b(y) \\ &+ \frac{1}{4\pi}\int_{\theta=0}^{\pi}\int_{\psi=0}^{2\pi} \sigma_s(\pi-\theta_i)I(y, \theta_i, \psi_i)\Phi(\theta_i, \psi_i, \theta, \psi) \\ &\times \sin\theta_i\,\mathrm{d}\psi_i\,\mathrm{d}\theta_i + \frac{\sigma_s(\pi-\theta_c)}{4\pi} q_0 e^{-\beta y/\mu_c}\,\Phi(\theta_c, \pi, \theta, \psi) \\ &+ \rho^s \frac{\sigma_s(\theta_c)}{4\pi} q_0 e^{-(2\tau_0-\beta y)/\mu_c}\,\Phi(\pi-\theta_c, \pi, \theta, \psi)\end{aligned} \tag{3}$$

The nonzero incidence angle θ_c causes intensity to be azimuthally-dependent, in addition to dependence on spatial position and directional polar angle.

The absorption efficiency used in Eq. (3) is shown in Fig. 1 as a function of emitted polar angle and the ratio of absorber diameter to lens diameter, after the analysis of Mackowski and Jones.[1] The absorption efficiency is azimuthally symmetric. The absorption efficiencies in Fig. 1 are calculated for a refracting material (lens sphere) with an index of refraction of 2 (corresponding to infrared transmitting materials such as sapphire or zinc selenide), and an absorbing material (embedded sphere) with a complex index of refraction of $2 + i$ (e.g., graphite). In each case in Fig. 1, the lens sphere has a particle size parameter $\pi d_p/\lambda = 30$, which is large enough to remove most of the size parameter dependence of absorption efficiency, and may be considered to be a gray limit. The ratio of absorber size parameter to lens size parameter (diameter ratio γ) is varied from 0.025 to 0.5. The extinction efficiency for these compound particles is constant at 2.2. The scattering phase function is calculated for the simple lens sphere from Lorenz/Mie theory, and is also taken to be a representative spectral average. The quadruple argument of the scattering phase function in Eq. (3) is resolved into a single argument by

$$\begin{aligned}\Phi(\theta_i, \psi_i, \theta, \psi) &\equiv \Phi(\Theta) \\ \cos\Theta &= \cos\theta\cos\theta_i + \sin\theta\sin\theta_i\cos(\psi-\psi_i)\end{aligned} \tag{4}$$

Since the environment is taken to be cold and the diffuse I does not explicitly include the collimated incident intensity, the incident surface boundary condition for Eq. (3) is

$$I(0, \theta|\theta < \pi/2, \psi) = 0 \tag{5}$$

while the specularly reflecting, diffusely emitting boundary condition on the collecting surface is

$$I(\tau_0/\beta, \theta|\theta > \pi/2, \psi) = \rho^s I(\tau_0/\beta, \pi - \theta, \psi) + (1 - \rho^s) I_b(\tau_0/\beta) \tag{6}$$

By following a standard approach for calculating the divergence of radiative flux from Eq. (2), excepting that directional dependence of the absorption and scattering coefficients is enforced, conservation of energy may be expressed

$$-k\nabla^2 T(\mathbf{r}) + \frac{\sigma_b}{\pi} T(\mathbf{r})^4 \int_{4\pi} \kappa(\hat{s})\, d\Omega - \int_{4\pi} \kappa(\hat{s}') I(\mathbf{r}, \hat{s})\, d\Omega - \kappa(\hat{s}_c') q_0 e^{-\tau/\mu_c} - \rho^s \kappa(\hat{s}_r') q_0 e^{-(2\tau_0 - \tau)/\mu_c} = 0 \tag{7}$$

Note that Eq. (7) includes effects of both the diffuse portion of the intensity I, as well as the nonextinct remnant of the direct and reflected collimated incident flux. Equation (7) is expressed for a plane parallel medium by

$$-k \frac{\partial^2 T(y)}{\partial y^2} + 2\sigma_b T(y)^4 \int_0^{\pi} \kappa(\theta) \sin\theta\, d\theta - \int_{\theta=0}^{\pi} \int_{\psi=0}^{2\pi} \kappa(\pi - \theta) \sin\theta\, I(y, \theta)\, d\psi\, d\theta - \kappa(\pi - \theta_c) q_0 e^{-\beta y/\mu_c} - \rho_s \kappa(\theta_c) q_0 e^{-(2\tau_0 - \beta y)/\mu_c} = 0 \tag{8}$$

Since the incident surface faces a cold vacuum while radiative flux is continuous across this surface, the appropriate boundary condition for Eq. (8) at $y = 0$ is a zero temperature gradient. Various boundary conditions may be applied at $y = y_{\max}$, depending on the operation of the heat exchange mechanism on the opposite side. A fixed temperature boundary condition is easily applied. However, for fixed heat flux boundary conditions where the collecting surface temperature is a variable, numerical solution makes it convenient to express the relation between boundary flux and temperature

$$q_w = (1 - \rho^s) \int_{\theta=0}^{\pi/2} \int_{\psi=0}^{2\pi} I(y_{\max}, \theta, \psi) \cos\theta \sin\theta\, d\theta\, d\psi - (1 - \rho^s)\sigma_b T_w^4 + (1 - \rho^s) q_0 \mu_c e^{-\tau_0/\mu_c} - k \left.\frac{\partial T}{\partial y}\right|_{y_{\max}} \tag{9}$$

where the first term is the incident and specularly reflected diffuse intensity, the second term is emission from the surface, the third term is the absorption of the attenuated collimated incidence, and the fourth term is conductive flux.

Equations (3) and (8) are discretized for numerical solution using a finite volume, finite solid angle approach to the discrete ordinates method as follows for the RTE:

$$\cos\theta_m \delta_j (I_{j,m,n}) + \beta I_{j,m,n} \delta_j(y) = \kappa_m I_{b,j} \delta_j(y) + \frac{\delta_j(y)}{4\pi} \sum_{m'=1}^{M} \sigma_{s,M-m'+1} w_{m'} \sum_{n'=1}^{N} I_{j,m',n'} \Phi_{m',n',m,n} w_{n'} - \frac{\mu_c \sigma_s(\pi - \theta_c)}{4\pi\beta} q_0 \delta_j(e^{-\beta y/\mu_c}) \Phi(\theta_c, \pi, \theta_m, \psi_n) + \rho^s \frac{\mu_c \sigma_s(\theta_c)}{4\pi\beta} q_0 \delta_j[e^{-(2\tau_0 - \beta y)/\mu_c}] \Phi(\pi - \theta_c, \pi, \theta_m, \psi_n) \tag{10}$$

and energy equation

$$-k\delta_j\left(\frac{\partial T}{\partial y}\right) + 8\sigma_b T_j^{*3} \delta_j(y) T_j \sum_{m=1}^{M} \kappa_m w_m = 6\sigma_b T_j^{*4} \delta_j(y) \sum_{m=1}^{M} \kappa_m w_m + \delta_j(y) \sum_{m=1}^{M} \sum_{n=1}^{N} \kappa_{M-m+1} I_{j,m,n} w_m w_n - \kappa(\pi - \theta_c) q_0 \frac{\mu_c}{\beta} \delta_j(e^{-\beta y/\mu_c}) + \rho^s \kappa(\theta_c) q_0 \frac{\mu_c}{\beta} \delta_j[e^{-(2\tau_0 - \beta y)/\mu_c}] \tag{11}$$

where the notation $\delta_j(y)$ implies $y_{j+1/2} - y_{j-1/2}$ and $\delta_j(\partial T/\partial y) = (T_{j+1} - T_j)/(y_{j+1} - y_j) - (T_j - T_{j-1})/(y_j - y_{j-1})$, and T^* is a linearization point. For specified heat flux boundary conditions at the collecting surface, Eq. (9) must be discretized and T_w must be solved in terms of q_w and $T(y)$, with the result added to the overall problem matrix. Otherwise, iterative solution for the unknown T_w is found to diverge.

For a plane parallel medium, a polar quadrature for discretization of the RTE would normally be chosen to satisfy as many forward moments of the intensity as the order of the quadrature, and equal integration weights would be employed for numerical stability. This procedure results in quadratures that are skewed away from the polar axis. In the present problem, there is great variation in the absorption coefficient and the scattering phase function near the polar axis, and so an opposite polar quadrature must be chosen that has fine divisions near the polar axis. However, choice of such a quadrature must result in highly nonuniform integration weights, which may lead to numerical instability. In the face of this difficulty, an ad hoc polar quadrature is chosen with equally distributed ordinates, $\theta_m = \pi(m - \frac{1}{2})/M$, and moderately unequal weights, $w_m^* = \pi \sin\theta_m/M$, where the weights are slightly adjusted so that the zeroth and first moments are satisfied:

$$a \sum_{m=1}^{M/4} w_m^* + b \sum_{m=M/4+1}^{M/2} w_m^* = 1$$
$$a \sum_{m=1}^{M/4} \cos\theta_m\, w_m^* + b \sum_{m=M/4+1}^{M/2} \cos\theta_m\, w_m^* = \frac{1}{2} \tag{12}$$

and then $w_m = a w_m^*$ for $m \le M/4$, and $w_m = b w_m^*$ for $m > M/4$. For a 16th-order quadrature ($M = 32$), $a = 0.9955$ and $b = 1.0013$. The azimuthal quadrature is taken as a simple equal angle $[\psi_n = 2\pi(n - \frac{1}{2})/N]$, equal weight ($w_n = 2\pi/N$) quadrature, as there is comparatively little intensity variation in the azimuthal direction. Care must be taken to renormalize the scattering phase function for each ordinate (m, n), so that

$$\frac{1}{4\pi} \sum_{m'=1}^{M} \sum_{n'=1}^{N} \Phi(\theta_{m'}, \psi_{n'}, \theta_m, \psi_n) w_{m'} w_{n'} = 1 \tag{13}$$

Equations (10) and (11) are solved with a nested iteration algorithm. Starting from a uniform temperature profile estimate $T(y) = (q_0/\sigma_b)^{1/4}$, and an intensity estimate $I = \sigma_b T^4/\pi$ to form the scattering term, the RTE is solved with a marching algorithm starting from incoming directions on the incident surface, proceeding to the far wall, reflecting, and solving outgoing intensities back to the incident surface. A uniform spatial mesh is employed, and diamond differencing (linear projection of intensity across each discrete cell) is used to project intensity values to the far side of the finite volume cells. The scattering term is then reformed and the marching algorithm is iterated, using the scattering term as the index

of convergence for this inner (RTE) iteration. This intensity field is then used in the linearized energy equation, which is solved with the Thomas (tridiagonal) algorithm. This temperature field is returned to the RTE routine for another complete inner (intensity) iteration to convergence, and forms the linearization point for the next outer (energy) iteration. Note that intensity and temperature linearization effects are iterated together in the outer iteration, using the full temperature field as a convergence index, while the inner iteration is concerned only with converging the intensity field for a given temperature field. Both the temperature and intensity are successively over-relaxed, using acceleration coefficients of 1.5. This has the effect of reducing the number of iterations to a set convergence criterion by about 50% in both loops. There is some difficulty in the computations for the combination of low N_s and high τ_0. In these cases, heat transfer is primarily radiative, and the conductive structure of the central difference energy equation breaks down. Purely radiative cases should be solved with a radiative equilibrium energy equation, although it is possible to produce convergent results with the present formulation for small but finite N_s, using an acceleration coefficient of 1.0 and many iterations.

Since a uniform spatial mesh is employed, it is possible to conduct numerical experiments to determine the order of discretization error. The overall solution is found to have a first-order error in spatial discretization for most cases tested, indicating that accuracy of the first-order RTE dominates the solution rather than that of the second-order energy equation. Extrapolating to an asymptotic solution from increasing mesh size results, it is found that a 16-element spatial mesh produces results of 1% accuracy over a practical range of input parameters. Spatial mesh coarseness leads to slight underestimates in temperature results. The overall solution does not have a regular error in directional discretization because of the highly forward effects of the absorption coefficient and the scattering phase function, although meshes larger than 32 polar elements (16th order quadrature) begin to pick up a linear error behavior. A 32-element polar mesh is found to provide results within 1% of the extrapolated asymptote, with coarse directional meshes yielding an overestimate in temperature results. If $\theta_c \neq 0$, the RTE is azimuthally-dependent. A 32-element azimuthal mesh (yielding 32×32 total ordinates) is found to provide asymptotic results for small θ_c.

Although completely comparable results are not available in the literature for validation of the numerical solution, it is possible to validate the present solution in simplified cases where the directional variation of absorption coefficient is suppressed and the collimated incident flux is replaced with a constant temperature boundary condition. For this purpose, there is a large volume of literature addressing combined radiation and conduction in plane parallel media. Comparisons are made to (numerical resolutions of) exact exponential solutions leading to temperature profiles by Crosbie (as reported in Ratzel and Howell[12]) for nonscattering media with black walls, and by Yuen and Wong[13] for linearly anisotropically scattering media with gray walls. Agreement to within 1% across the slab is achieved in each case.

Results

The controlling parameters of the present problem are found by writing the energy equation in dimensionless form:

$$-4N_s \frac{\partial^2 \Gamma}{\partial \tau^2} + \frac{2\Gamma^4}{Q_c} \int_0^{\pi} Q_a(\theta) \sin\theta \, d\theta - \frac{1}{\pi Q_c} \int_{\theta=0}^{\pi} \int_{\psi=0}^{2\pi} Q_a(\pi - \theta) I^*(\tau, \theta, \psi) \sin\theta \, d\psi \, d\theta - \frac{Q_a(\pi - \theta_c)}{Q_c} e^{-\tau/\mu_c} - \rho^s \frac{Q_a(\theta_c)}{Q_c} e^{-(2\tau_0 - \tau)/\mu_c} = 0 \qquad (14)$$

suggesting that the results may be summarized by Γ as a function of $Q_a(\theta)$, N_s, τ_0, ρ^s, and θ_c, as well as the boundary conditions. For the one compound particle configuration considered here (embedded eccentric sphere), $Q_a(\theta)$ is specified by selecting γ (Fig. 1). As the best radiation trapping (effective absorptivity to emissivity ratio) performance is found with $\rho^s = 1$ for most cases (which enhances the multiple reflections of the radiation trapping effect), this parameter is fixed. (In cases involving nonspecular radiation leaving the collecting surface, intensity is less confined to the directionally narrow band of high absorption demonstrated by the compound particles (Fig. 1). Results for compound particle media with absorbing boundaries therefore show little advantage over media with simple (nondirectionally varying absorption coefficient) particles. A further parameter similar to θ_c is introduced by considering the potential difficulty of embedding the compound particles in the substrate with perfect orientation. If the orientation of the compound particles is considered to be a zero-mean Gaussian distributed random variable with standard deviation σ_θ, then the effective absorption coefficient distribution is defined by

$$\kappa^*(\theta) = \frac{1}{4\pi} \int_{\theta'=0}^{\pi} \int_{\psi'=0}^{2\pi} p(\theta') \kappa(\Theta) \sin\theta' \, d\psi' \, d\theta'$$

$$p(\theta') = \frac{1}{2\pi\sigma_\theta} \exp\left(-\frac{\theta'^2}{2\sigma_\theta^2}\right) \qquad (15)$$

$$\cos\Theta = \cos\theta \cos\theta' + \sin\theta \sin\theta' \cos(\psi - \psi')$$

where $\kappa^*(\theta)$ may be substituted for $\kappa(\theta)$ in Eqs. (3) and (8). [Care must be taken in discretization of $p(\theta')$ to retain proper normalization.]

One purpose of the proposed radiation trapping configuration might be to produce a high temperature on the collecting surface. Therefore, in the first results case, Γ_w is studied as a function of τ_0, γ, N_s, θ_c, and σ_θ for the limiting (and purely illustrative) case of an insulated collecting surface (no heat taken from the high-temperature reservoir). An opposite case, the second results case, is represented by the heat flux passing through the collecting surface resulting from a fixed temperature boundary condition.

Without the assumption of Kirchhoff's law, and with a directionally-dependent absorption coefficient, definition of either effective absorptivity or effective emissivity would require a whole system of special definitions and assumptions. Comparing the results of such a system with prior, Kirchhoffian, directionally-independent effective absorptivity results would be somewhat problematical. Instead, the performance of a compound particle medium bounded by a specularly reflecting surface is related, by analogy, to that of an opaque flat plate. An opaque flat plate under incident flux q_0 may reflect $[(1 - \alpha)q_0]$ or emit $(\varepsilon\sigma_b T_w^4)$ flux in the opposite direction of the incident flux, or flux may be passed through this plate $(\zeta_w q_0)$ by conduction/convection. An energy balance on the plate yields one equation, $\alpha = \zeta_w + \varepsilon\Gamma_w^4$, for the four unknowns.

In the first case considered, the surface is insulated ($\zeta_w = 0$), and so either variable, α/ε or Γ_w, may be determined, given the other. Neither α nor ε may be determined independently. If α/ε is known for some flat plate ($\alpha/\varepsilon = 1$ for a gray Kirchhoff surface), then Γ_w may be determined. If, on the other hand, solution of the radiative transfer and energy equations for the compound particle medium yields Γ_w directly, then the effective α/ε of the medium may be determined ($\alpha/\varepsilon = \Gamma_w^4$) and compared to the Kirchhoffian result ($\Gamma_w = 1$). The result holds regardless of the absolute magnitude of α or ε. In the second case considered, a temperature (or Γ_w) boundary condition is specified and the flux "absorbed" through the plate is calculated ($\zeta_w \neq 0$). If α/ε is known for some flat plate ($\alpha/\varepsilon = 1$ for a gray Kirchhoff

surface), then ζ_w may be determined given α. If $\Gamma_w = 1$, then $\zeta_w = 0$ for a gray Kirchhoff surface, regardless of α. If, on the other hand, solution of the radiative transfer and energy equations for the compound particle medium yield ζ_w directly, then this result may be compared to the Kirchhoffian result ($\zeta_w = 0$), although the relative contributions of α and ε cannot be distinguished. In summary, the performance of a compound particle medium, as a layer over an opaque, specularly reflecting surface, is compared to the two definitive cases for Kirchhoff surfaces: 1) where $\zeta_w = 0$ and any $\Gamma_w > 1$ represents an enhanced-absorptivity surface (Fig. 3), and 2) where $\Gamma_w = 1$ and any $\zeta_w > 0$ represents an enhanced-absorptivity surface (Figs. 4 and 5).

Figure 3 shows the results for the first case, demonstrating the absorption to emission performance of the substrate/compound particle medium in the limiting case of an insulated collecting surface by showing the variation of Γ_w with τ_0 for a range of γ, for normal incidence, perfect particle orientation, and $N_s = 0.1$. The medium is capable of providing an effective absorptivity to emissivity ratio of up to 70 ($\Gamma_w = 2.89$) for small γ and τ_0, demonstrating its utility as a radiation trap. Less of the incident flux penetrates to the collecting surface in optically thick cases. The collecting surface temperature decreases with increasing medium optical thickness in the insulated case due to increased scattering from particles near the incident surface. Unfortunately, this means that higher optical thicknesses, which have a higher effective absorptivity, and thus absorb more of the incident flux, are less efficient (have a lower effective absorptivity-to-emissivity ratio). This suggests that while high-quality (high-temperature) energy may be collected by compound particle media, high-quantity (high-flux through the collecting plate) might not be available

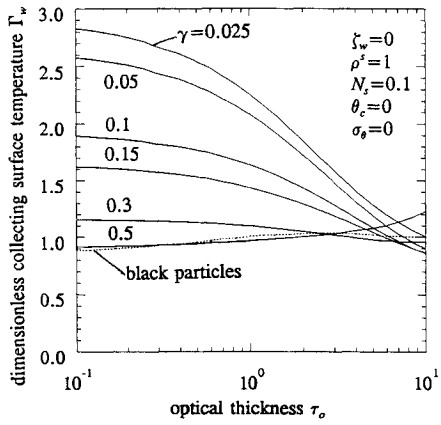

Fig. 3 Collecting surface temperature as function of optical thickness for insulated collecting surface.

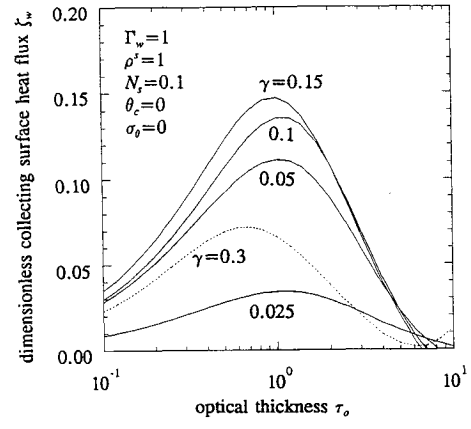

Fig. 4 Heat flux through collecting surface as function of optical thickness for $T_w = (q_0/\sigma_b)^{1/4}$, over range of γ_s.

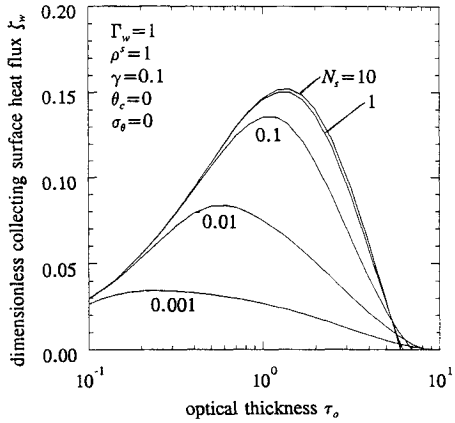

Fig. 5 Heat flux through collecting surface as function of optical thickness for $T_w = (q_0/\sigma_b)^{1/4}$, over range of N_s.

using the present compound particle configuration (simple eccentric spheres). It should be noted, however, that for large γ, Γ_w increases slightly with increasing τ_0, reaching a value of 1.56 ($\alpha/\varepsilon = 6$) at $\tau_0 = 100$, and suggesting a possible high-quality, high-quantity compromise. Figure 3 also shows Γ_w for black particles ($\gamma = 1$, no directional variation in absorption coefficient), indicating $\Gamma_w \approx 1$, and thus having no advantage over a Kirchhoff surface ($\Gamma_w = 1$).

The lack of a nonzero optimal τ_0 may be interpreted by considering that the unique directional scattering and absorption properties are primarily responsible for achieving $\Gamma_w > 1$, and any additional extinction caused by a finite optical thickness merely interferes with the transport of the incident flux to the reflecting surface. Therefore, the optimal optical thickness is just that minimum necessary to ensure that the properties of the particulate medium act in a uniform radiative continuum. The optical thickness of a single layer of closely packed particles (ignoring continuum considerations) is $\pi Q_e/4$, or 1.72 for the particles considered here, which is too high to give optimal performance. However, for disperse particle assemblies, it might be approximated that the minimum optical thickness for continuum is $15Q_e(d_p/s)^2$ (10 rows), where s is the mean interparticle spacing. Therefore, lower optical thickness (although higher dimensional thickness) and higher Γ_w may be achieved with more disperse media.

Comparing Fig. 3 with Fig. 1, it may be seen that compound particles with larger absorbing spheres (larger γ), and therefore, larger absorption efficiencies, produce lower effective absorptivity-to-emissivity ratios. This effect illustrates the importance of the perfectly reflective collecting surface in the radiation trapping effect. While the higher γ particles have higher absorption efficiencies, they also have a lower ratio of forward-to-backward absorption efficiency, with the result that the backwards emission cannot reach the collecting surface. Forward emitted power, however small, is available to enter the reflection/absorption/emission cycle between the compound particles and the collecting surface, while backwards emission is not. The indication is that while a high forward absorption efficiency is important, a low backward efficiency is even more so.

The results of Fig. 3 show little sensitivity to N_s, which is a consequence of the very flat temperature profiles found in these cases. For low τ_0, the temperature profiles are nearly flat, and there is no significant effect of N_s. For higher τ_0, there is some tendency toward a higher temperature at the collecting surface than at the incident surface. In these cases, a higher N_s leads to a slightly lower Γ_w, due to conductive leakage.

Figure 4 shows the second results case, in which the collecting surface temperature is fixed at $\Gamma_w = 1$, and results are given for the heat flux through the collecting surface. These results are also for normal incidence, perfect particle orien-

tation, $\rho^s = 1$, and $N_s = 0.1$. Since all radiative flux is reflected at the collecting surface to maintain the radiation trapping effect, the net flux at the collecting surface is due entirely to conduction. Figure 4 shows that collected flux increases with increasing γ up to $\gamma = 0.15$, confirming that while lower γ particles tend to produce higher temperatures in an insulated case, these high temperatures cannot be converted into a high flux due to their low overall absorption. For higher γ, Fig. 1 shows an increasing ratio of backwards-to-forwards absorption, with the result that more heat is emitted. For $\gamma = 1$, the particles are Kirchhoffian and $\zeta_w = 0$. The results indicate a finite optimal τ_0 of about unity for all γ. Smaller τ_0 have less potential to absorb, and larger τ_0 tend to produce an insulative effect between the incident flux and the collecting surface. The highest ζ_w achieved in Fig. 4 is 0.15, so that 15% of the incident flux is passed by conduction through the collecting surface if it is maintained at $\Gamma_w = 1$. Under the condition of $\Gamma_w = 1$, a gray, Kirchhoffian plate has a through-flux of zero. The compound particle medium demonstrates a positive, nonzero through-flux for most parameter combinations. The compound particle medium, therefore, demonstrates performance superior to that of a Kirchhoffian plate in this case.

While the presence of conduction does little to enhance the collecting surface temperature in the insulated case, higher conductivity is useful for enhancing heat flux in the fixed temperature boundary condition case. Figure 5 shows the effect of N_s on the ζ_w vs τ_0 relation for $\gamma = 0.1$. Increasing N_s increases thermal conductivity, which increases conductive heat flux. Since $\rho^s = 1$ is necessary to set the radiation trap, conduction is the only mechanism for passing heat through

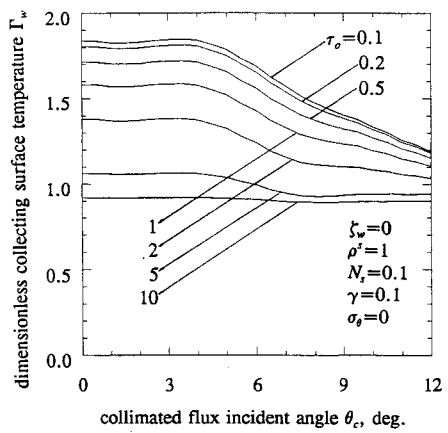

Fig. 6 Collecting surface temperature as function of collimated flux incidence angle for insulated collecting surface.

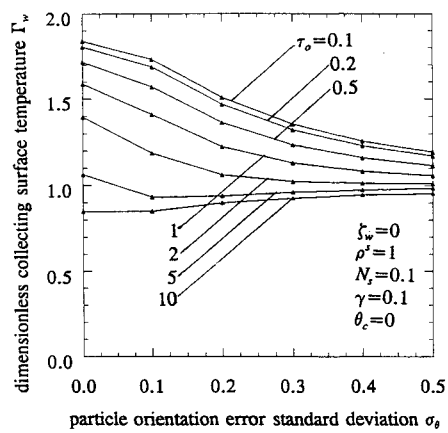

Fig. 7 Collecting surface temperature as function of compound particle orientation error standard deviation for insulated collecting surface.

the collecting surface. In general, it appears that $N_s > 1$ is beneficial, although increasing N_s much beyond unity produces only diminishing returns. It should be noted that the optimal parameter values indicated by Fig. 5, $\tau_0 = 1$ and $N_s = 1$, may be achieved by a slab subject to a low Earth orbit solar constant by $k/y_{max} = 0.14$ W/m^{2}K. This is realizable using very ordinary materials and moderate thicknesses.

For smaller γ, Fig. 1 shows that the polar range of higher absorption efficiency is fairly limited. Collimated incident flux from angles outside this range is less able to enter the reflection/absorption/emission system between the reflective surface and the particles, producing less favorable results. Figure 6 shows the variation of Γ_w with θ_c for an insulated collecting surface, perfectly oriented particles, $N_s = 0.1$, $\gamma = 0.1$, and a range of τ_0. Figure 1 shows that there is little change in the absorption efficiency for $\gamma = 0.1$ for θ_c up to about 4 deg, and Fig. 6 reflects this result with little change in Γ_w. However, for $\theta_c > 4$ deg, Γ_w is reduced, and for $\theta_c > 12$ deg, the reduction is great enough that there is little advantage to using the $\gamma = 0.1$ compound particles. It appears that while the substrate/compound particle medium can tolerate a large error in incident flux pointing accuracy, on the order of 4 deg, this medium might not be useful in passive collection systems.

Figure 7 examines the sensitivity to compound particle orientation error of insulated collecting surface results for $\gamma = 0.1$, $N_s = 0.1$, and normal incidence. In Fig. 7, the $\sigma_\theta = 0$ results are for perfect orientation, while the $\sigma_\theta \neq 0$ results include the application of Eq. (15). For optically thin media, the sensitivity of the collecting surface temperature to σ_θ is of similar order to the sensitivity to θ_c shown in Fig. 6, as increasing σ_θ decreases the ability of the compound particles to trap rays of intensity. For optically thick media, increased σ_θ actually improves Γ_w, as there is a slightly increased ability of the particles to absorb backscattered intensity. It appears that the substrate/compound particle medium requires particle orientation to be nominally correct (within, e.g., 6 deg), but that highly precise manufacturing might not be required.

Conclusions

A particular configuration is proposed that employs a class of compound particles, themselves proposed in another work, which have the characteristic of directionally varying absorption and scattering efficiencies. The proposed configuration embeds a disperse layer of these compound particles in a conducting, radiatively nonparticipating substrate, with one side exposed to collimated flux and the other side bounded by an opaque, specularly reflecting surface. The compound particles are oriented so as to be highly absorbing in the direction towards the reflective surface, and highly scattering in the direction towards the incidence. It is found through the numerical solution of directionally varying absorption coefficient forms of the RTE and energy conservation equation that a radiation trap is developed that can build up temperatures corresponding to an effective absorptivity-to-emissivity ratio of up to 70. The maximum heat flux passing through the layer is only 15% of the incident flux, although this is calculated in a setting where no flux at all would pass through a gray surface that obeys Kirchhoff's law. While the proposed configuration could be immediately useful for the development of high temperatures under direct flux, further development of the compound particle characteristics may be necessary for applications calling for a high heat flux passing through the collecting surface. A device based on the proposed enhanced absorption surface must track the source of collimated incident flux, although the required tracking accuracy is not severe. The proposed configuration must also be manufactured so that the compound particles have a uniform orientation, although the sensitivity to random orientation error is not extreme.

In general, it appears that continued development of compound particles with directionally varying absorption and scat-

tering efficiencies would be worthwhile, in terms of both analytical development and development of fabrication techniques. Further development of compound particles for use in flux absorption devices should concentrate on particles that have a high ratio of forward absorption efficiency to backward absorption efficiency. In high-temperature generation applications, this ratio is found to be more important than a high absorption efficiency, per se, in any particular direction.

References

[1]Mackowski, D. W., and Jones, P. D., "Theoretical Investigation of Particles Having a Directionally-Dependent Absorption Cross Section," *Journal of Thermophysics and Heat Transfer*, Vol. 9, No. 2, 1995, pp. 193–201.

[2]Howell, J. R., "Thermal Radiation in Participating Media: the Past, the Present, and Some Possible Futures," *Journal of Heat Transfer*, Vol. 110, No. 4(B), 1988, pp. 1220–1229.

[3]Lee, S. C., "Radiative Transfer Through a Fibrous Medium: Allowance for Fiber Orientation," *Journal of Quantitative Spectroscopy and Radiative Transfer*, Vol. 36, No. 3, 1986, pp. 253–263.

[4]Lee, S. C., "Effect of Fiber Orientation on Thermal Radiation in Fibrous Media," *International Journal of Heat and Mass Transfer*, Vol. 32, No. 2, 1989, pp. 311–319.

[5]Lee, S. C., "Scattering Phase Function for Fibrous Media," *International Journal of Heat and Mass Transfer*, Vol. 33, No. 10, 1990, pp. 2183–2190.

[6]Chern, B.-C., Moon, T. J., and Howell, J. R., "Angle-of-Incidence Dependent Scattering Effects in Arrays of Parallel Cylinders Typical of Tape-Wound Composites," *Radiative Heat Transfer: Current Research*, edited by Y. Bayazitoğlu, A. L. Crosbie, P. D. Jones, R. D. Skocypec, T. F. Smith, T. W. Tong, and S. T. Thynell, American Society of Mechanical Engineers, HTD-Vol. 276, New York, 1994, pp. 79–90.

[7]Marshak, A. L., "The Effect of the Hot Spot on the Transport Equation in Plant Canopies," *Journal of Quantitative Spectroscopy and Radiative Transfer*, Vol. 42, No. 6, 1989, pp. 615–630.

[8]Shultis, J. K., and Myneni, R. B., "Radiative Transfer in Vegetation Canopies with Anisotropic Scattering," *Journal of Quantitative Spectroscopy and Radiative Transfer*, Vol. 39, No. 2, 1988, pp. 115–129.

[9]Myneni, R. B., Asrar, G., and Kanemasu, E. T., "Finite Element Discrete Ordinates Method for Radiative Transfer in Non-Rotationally Invariant Scattering Media: Application to the Leaf Canopy Problem," *Journal of Quantitative Spectroscopy and Radiative Transfer*, Vol. 40, No. 2, 1988, pp. 147–155.

[10]Modest, M. F., *Radiative Heat Transfer*, McGraw-Hill, New York, 1993.

[11]Kim, T.-K., and Lee, H. S., "Radiative Transfer in Two-Dimensional Anisotropic Scattering Media with Collimated Incidence," *Journal of Quantitative Spectroscopy and Radiative Transfer*, Vol. 42, No. 3, 1989, pp. 225–238.

[12]Ratzel, A. C., and Howell, J. R., "Heat Transfer by Conduction and Radiation in One-Dimensional Planar Media Using the Differential Approximation," *Journal of Heat Transfer*, Vol. 104, No. 2, 1982, pp. 388–391.

[13]Yuen, W. W., and Wong, L. W., "Heat Transfer by Conduction and Radiation in One-Dimensional Absorbing, Emitting and Anisotropically-Scattering Medium," *Journal of Heat Transfer*, Vol. 102, No. 2, 1980, pp. 303–307.

Progress in Turbulence Research

Herman Branover and Yeshajahu Unger, Editors, Ben-Gurion University of the Negev, Beer-Sheva, Israel

This volume contains a collection of reviewed and revised papers devoted to modern trends in the research of turbulence from the Seventh Beer-Sheva International Seminar on MHD Flows and Turbulence, Ben-Gurion University of the Negev, Beer-Sheva, Israel, February 14-18, 1993.

Progress in Astronautics and Aeronautics
1994, 348 pp, illus, Hardback
ISBN 1-56347-099-3
AIAA Members $69.95
Nonmembers $99.95
Order #: V-162

Place your order today! Call 1-800/682-AIAA

CONTENTS:
Preface • Turbulence: A State of Nature or a Collection of Phenomena? • Probability Distributions in Hydrodynamic Turbulence • Model of Boundary-Layer Turbulence • Some Peculiarities of Transfer and Spectra in a Random Medium with Reference to Geophysics • Magnetohydrodynamic Simulation of Quasi-Two-Dimensional Geophysical Turbulence • Two-Dimensional Turbulence: Transition • Two-Dimensional Turbulence: The Prediction of Coherent Structures by Statistical Mechanics • Large-Scale Dynamics of Two-Dimensional Turbulence with Rossby Waves • Suppression of Bubble-Induced Turbulence in the Presence of a Magnetic Field • Transition to Weak Turbulence in a Quasi-One-Dimensional System • Magnetohydrodynamic Rapid Distortion of Turbulence • Inertial Transfers in Freely Decaying, Rotating, Stably Stratified, and Magnetohydrodynamic Turbulence • Heat Transfer Intensification to the Problem When the Velocity Profile Is Deformed • Magnetohydrodynamic Heat Transfer Intensification to the Problems of Fusion Blankets • Spontaneous Parity Violation and the Correction to the Kolmogorov Spectrum • Turbulence Energy Spectrum in Steady-State Shear Flow • Structure of the Turbulent Temperature Field of a Two-Dimensional Fire Plume • Development of a Turbulent Wake Under Wall Restricting and Stretching Conditions • Renormalization of Ampere Force in Developed Magnetohydrodynamic Turbulence • Algebraic $Q4$ Eddy-Viscosity Model for Near-Rough-Wall Turbulence • Group Analysis for Nonlinear Diffusion Equation in Unsteady Turbulent Boundary-Layer Flow • Numerical Simulations of Cylindrical Dynamos: Scope and Method • Convective-Type Instabilities in Developed Small-Scale Magnetohydrodynamic Turbulence • Flux Tube Formation Due to Nonlinear Dynamo of Magnetic Fluctuations • Relaxation to Equilibrium and Inverse Energy Cascades in Solar Active Regions • Use of k-ε Turbulence Model for Calculation of Flows in Coreless Induction Furnaces

AIAA
American Institute of Aeronautics and Astronautics
Publications Customer Service, 9 Jay Gould Ct., P.O. Box 753, Waldorf, MD 20604
FAX 301/843-0159 Phone 1-800/682-2422 8 a.m. - 5 p.m. Eastern

Sales Tax: CA residents, 8.25%; DC, 8%. For shipping and handling add $4.75 for 1-4 books (call for rates for higher quantities). Orders under $100.00 must be prepaid. Foreign orders must be prepaid and include a $25.00 postal surcharge. Please allow 4 weeks for delivery. Prices are subject to change without notice. Returns will be accepted within 30 days. Non-U.S. residents are responsible for payment of any taxes required by their government.